Jurnal Sainstech Nusantara	Vol. 2 No. 3 (2025) 57-66
https://nusantarajournal.id/sainstech	ISSN: 3063-0657

Optimization Control in MG-16 DC Motor Using LQR and LQT Configurations

Anggara Trisna Nugraha[1], Muhammad Bilhaq Ashlah[2], Rama Arya Sobhita[1], Dhadys Ayu Juli Anjhani[3]

[1]Marine Electrical Engineering, Shipbuilding Institute of Polytechnic Surabaya, Indonesia
[2]Bio-Industrial Mechatronics Engineering, National Chung Hsing University, Taiwan
[3]Design and Manufacture Engineering, Shipbuilding Institute of Polytechnic Surabaya, Indonesia

Article Info

Article history:

Received 11 May, 2025
Revised 15 July, 2025
Accepted 18 August, 2025

Abstract

DC motors are widely used electronic components commonly found in everyday applications. Typically, when a load is applied, a DC motor tends to decelerate and fails to maintain a constant speed. To address this, motor speed can be controlled by adjusting the input voltage. However, to maintain consistent speed under varying loads, a control system is necessary. LQR works by adjusting the motor response to closely approach the desired setpoint, while minimizing both overshoot and undershoot within the system. On the other hand, LQT is a linear control strategy designed to ensure that the system output closely follows a time-varying reference or setpoint. When implemented, LQR yields a motor response that aligns with the target setpoint without any overshoot or undershoot. In contrast, if LQR is not applied, the motor response deviates significantly from the desired target and takes a longer time to settle. Meanwhile, the LQT method produces a quicker response reaching steady state in approximately ±0.5 seconds although it does introduce some overshoot and slight ripple in the signal. Despite these minor drawbacks, LQT is often favored over LQR for applications involving the MG-16B DC motor due to its superior speed in reaching the setpoint.

Keyword: LQR, LQT, Motor DC, Noise, Optimation.

Corresponding Author:

Name: Anggara Trisna Nugraha
Email: anggaranugraha@ppns.ac.id

1. Introduction

DC motors are among the most widely used electromechanical actuators in various industrial and technological applications. These motors operate based on electromagnetic principles, wherein the interaction between the magnetic fields of the rotor and stator produces a repulsive force that

DOI: https://doi.org/10.71225/jstn.v2i3.105

drives rotation. When electric current flows through the armature windings, it generates a magnetic field that induces mechanical motion proportional to the input voltage. However, DC motors inherently tend to decelerate under varying load conditions, resulting in non-constant rotational speeds. Therefore, precise speed regulation is essential to ensure consistent motor performance, particularly under fluctuating loads.

In control systems, the primary function of a controller is to compare the actual system output with the reference input (setpoint), calculate the resulting error, and produce a control signal that minimizes this error. To achieve optimal control performance, strategies are required that can maintain system stability, accuracy, and responsiveness, even in the presence of disturbances.

Two widely recognized optimal control methods employed to improve DC motor performance are the Linear Quadratic Regulator (LQR) and the Linear Quadratic Tracker (LQT). LQR is a state-feedback control technique designed to minimize a quadratic cost function, thereby yielding a fast and stable system response without overshoot or undershoot. It is particularly effective in multi-input multi-output (MIMO) systems due to its efficiency and robustness. In contrast, LQT extends the LQR approach by incorporating a feedforward term that enables the system output to follow a time-varying reference trajectory. This method combines conventional linear feedback with reference-based optimization, making it suitable for tracking applications.

This study investigates and compares the effectiveness of LQR and LQT in regulating the speed of a DC motor model (RS 550 type). Simulations were conducted using MATLAB and Simulink to model the control system and analyze its output response. Additionally, noise was introduced into the system to evaluate how well each control method maintains performance under external disturbances. The findings provide insight into the robustness and adaptability of each method when applied to dynamic and non-linear system conditions.

2. Research Method

2.1. DC Motor Identification

At this stage, identification is carried out regarding the specifications of the DC Motor that will be researched. The form of the DC Motor that was researched was a brushless motor with the name and type MG-16B. The following is the datasheet of the MG-16B DC Motor.

Gear Ratio	Rated Voltage	Part Number	Torque (mNm)			Speed (nin^{-1}) (Reference)		Current (mA)			Length (mm)		Weight (g) (Reference)
			Rated	Max.	Starting	No-Load	Rated	No-Load	Rated	Starting	Motor	Gear	
1/30	DC6 V	MG16B-030-AA-00	20	30	> 50	477	380	< 160	< 400	< 1600	35	14	25
	DC12 V	MG16B-030-AB-00						< 80	< 250	< 800			
1/60	DC6 V	MG16B-060-AA-00	40	60	> 100	213	160	< 160	< 400	< 1600	38	17	30
	DC12 V	MG16B-060-AB-00						< 80	< 250	< 800			
1/120	DC6 V	MG16B-120-AA-00	60	90	> 170	127	100	< 160	< 400	< 1600			
	DC12 V	MG16B-120-AB-00						< 80	< 250	< 800			
1/240	DC6 V	MG16B-240-AA-00	120	180	> 350	53	40	< 160	< 400	< 1600	41	20	35
	DC12 V	MG16B-240-AB-00						< 80	< 250	< 800			
1/300	DC6 V	MG16B-300-AA-00	160	240	> 400	45	34	< 160	< 400	< 1600			
	DC12 V	MG16B-300-AB-00						< 80	< 250	< 800			

Figure 1. Datasheet Motor DC MG-16B

DOI: https://doi.org/10.71225/jstn.v2i3.105

The second order DC motor model can be written mathematically as follows.

$$G(s) = \frac{\omega n^2}{s^2 + 2\varsigma\omega n s + \omega n^2} \quad (1)$$

Description:
ζ = Damping Ratio (dB)
ωn = Natural Frequency (rad/s)

Where:

$$\omega n = 2\pi f \quad (2)$$

$$\omega n = 2 \times 3{,}14 \times 50 = 314 \text{ rad/s}$$

So the calculation of the MG-16B DC motor based on the specifications from the datasheet obtained is:

$$G(s) = \frac{\omega n^2}{s^2 + 2\varsigma\omega n s + \omega n^2} \quad (3)$$

$$G(s) = \frac{2\pi f^2}{s^2 + 2\varsigma(2\pi f)s + 2\pi f^2} \quad (4)$$

$$(s) = \frac{2\pi 50^2}{s^2 + 2.30.(2\pi 50)s + 2\pi 50^2} \quad (5)$$

$$G(s) = \frac{98596}{s^2 + 18840s + 98596} \quad (6)$$

2.2. Linear Quadratic Regulator (LQR)

The Linear Quadratic Regulator (LQR) is a technique widely employed in modern control theory. This method analyzes system behavior through the state-space approach. Due to the simplicity and efficiency of this framework, it is particularly well-suited for systems with multiple inputs and outputs (MIMO). In general, the state-space representation of such a system can be formulated as follows:

$$\dot{X} = AX + Bu \quad (7)$$

In principle, the LQR method searches for a control signal u that minimizes the performance index J.

$$J = \int (X^T Q_x + u^T R_a) dt \quad (8)$$

LQR finds the optimal control input law u*. The constraints imposed by the Q and R matrices minimize the performance index. The closed-loop optimal control law is defined as:

$$u^* = -Kx \quad (9)$$

Here, K represents the optimal feedback gain matrix. This gain matrix is designed to minimize the performance index by appropriately placing the closed-loop poles to achieve the desired system behavior. The feedback gain matrix K is determined based on the matrices A, B, Q, and R. To compute K, the Algebraic Riccati Equation (ARE) must be solved. The matrix P, which is symmetric and positive definite, is the solution to the ARE and is defined as:

$$A^T P + PA - PBR^{-1}B^T P + Q = 0 \quad (10)$$

$$K = AX - BKx = (A - BK)x \quad (11)$$

DOI: https://doi.org/10.71225/jstn.v2i3.105

By substituting equations (8) and (9), the expression becomes:

$$x = AX - BKx = (A - BK)x \quad (12)$$

The block diagram illustrating the LQR configuration is shown in Figure 2.

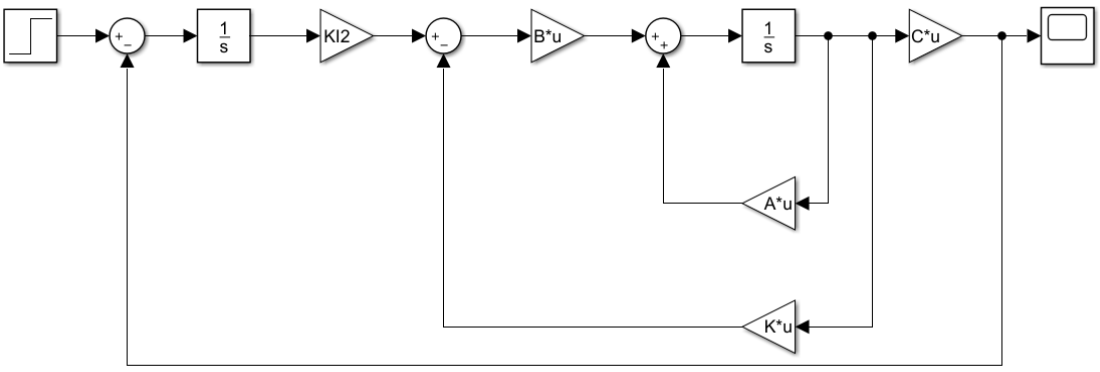

Figure 2. Block diagram LQR

2.3. Linear Quadratic Tracker (LQT)

The LQT consists of the usual state feedback of a linear dynamic system together with an additional feed-forward control term. The feed-forward control term depends on the reference signal vector, r(t). The vector r(t) is given by:

$$r(t) = [V_{ref}(t)\ \ 0]^T \quad (13)$$

Where, Vref is a time-varying reference voltage signal. The LQT scheme minimizes the squared performance index to produce the optimal control decision which can be formulated in the following equation.

$$J = \frac{1}{2}\int_0^T [(x(t) - r(t))^T Q\big(x(t) - r(t)\big) + d(t)^T R d(t)]dt \quad (14)$$

Where, Q and R are the intermediate state and control weighting matrices, respectively. They are chosen such that; Q = QT ≥ 0 and R = RT > 0. Due to the quadratic nature of the cost function, the control signal is proportional to the quadratic variation of the equation. Thus, if the state-variations are large; minimization and, hence, the convergence rate is faster. The optimal affine control decision is evaluated through the mathematical expression shown in

$$d(t) = -Kx(t) + K_{ff} v_{ref}(t) \quad (15)$$

Where,

$$K = R^{-1}B^T P \quad (16)$$

$$K_{ff} = R^{-1}B^T((A - BK)^T)^{-1}H^T Q \quad (17)$$

DOI: https://doi.org/10.71225/jstn.v2i3.105

The gain vector, K, helps to relocate the system poles to synthesize the optimal controller. The optimal gain vector depends on the symmetric positive definite matrix, P, shown in equation (14). The matrix, P, for a given system can be obtained by solving the Riccati Algebra Equation, shown in.

$$A^T P + PA - PBR^{-1}B^T P + H^T \mathrm{QH} = 0 \quad (18)$$

The block diagram showing the LQR configuration is shown in Figure 3.

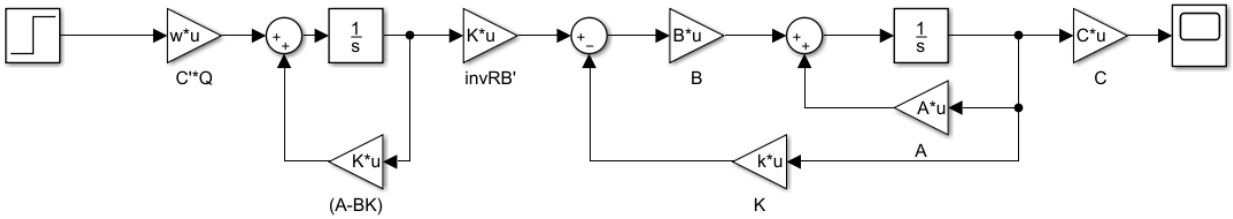

Figure 3. Block diagram LQT

2.4. Block Diagram System

The motor block diagram aims to determine the original response results of the DC motor if the MG-16B DC motor is not added to the method used in the Simulink software.

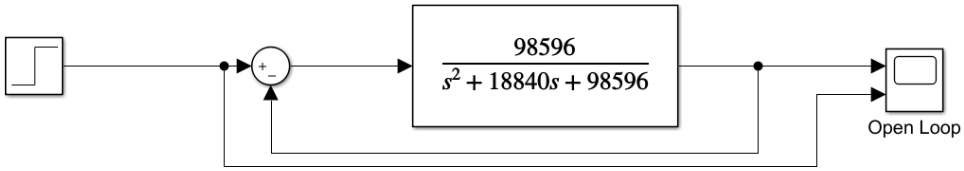

Figure 4. Block diagram DC Motor

Figure 4 shows a second-order block diagram of a DC motor consisting of an input and an output. The input used is a step response type. The transfer function in the diagram can contain a second-order DC motor modeling. The response results will be displayed on the scope and display to find out the maximum response value produced.

- Subsystem block diagram LQR in DC motor MG-16B

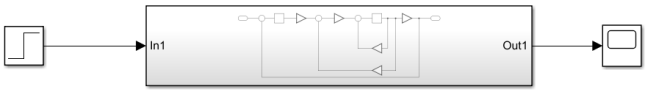

Figure 5. Subsystem block diagram LQR in DC motor MG-16B

- Subsystem block diagram LQR in DC motor MG-16B with noise

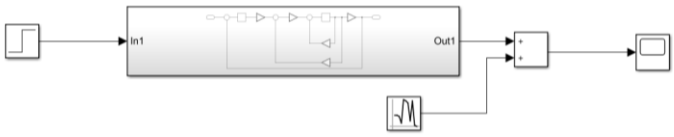

Figure 6. Subsystem block diagram LQR in DC motor MG-16B with noise

DOI: https://doi.org/10.71225/jstn.v2i3.105

- Subsystem block diagram LQT in DC motor MG-16B

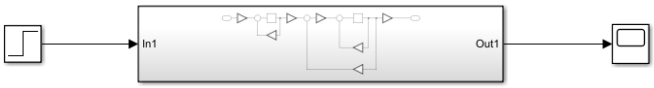

Figure 7. Subsystem block diagram LQT in DC motor MG-16B

- Subsystem block diagram LQT in DC motor MG-16B

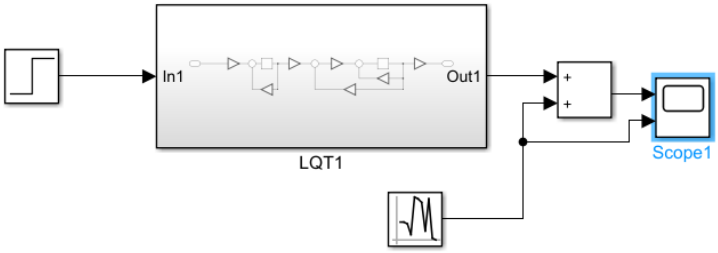

Figure 8. Subsystem block diagram LQT in DC motor MG-16B with noise

3. Results And Discussion

This section discusses the results of the MG-16B DC motor response in the first-order mathematical model and when given the LQR and LQT methods with and without noise. The response results were obtained using simulations in the Simulink Matlab software.

3.1. Second Order Response Results of MG-16B DC Motor

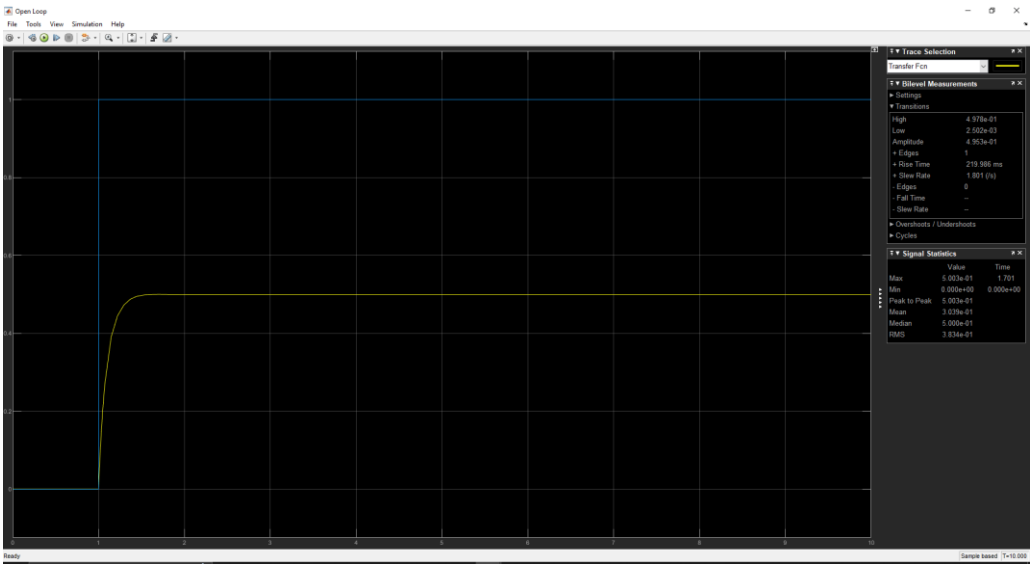

Figure 9. Second Order Response Results of MG-16B DC Motor

In the second-order modal response output seen in Figure 9, the second-order motor response graph shows that the output is very far from the desired set point. The yellow wave is the result of the motor response while the blue wave is the desired set point. The desired set point is 0.5 while the motor response is only at a value of 219 with high ripples in the motor response rise time.

DOI: https://doi.org/10.71225/jstn.v2i3.105

The observed MG-16B DC motor has linear characteristics as indicated by the signal shape that has no ripples. The motor response is in a steady state condition at ±0.27 seconds.

3.2. MG-16B DC Motor Response Results Using LQR Method

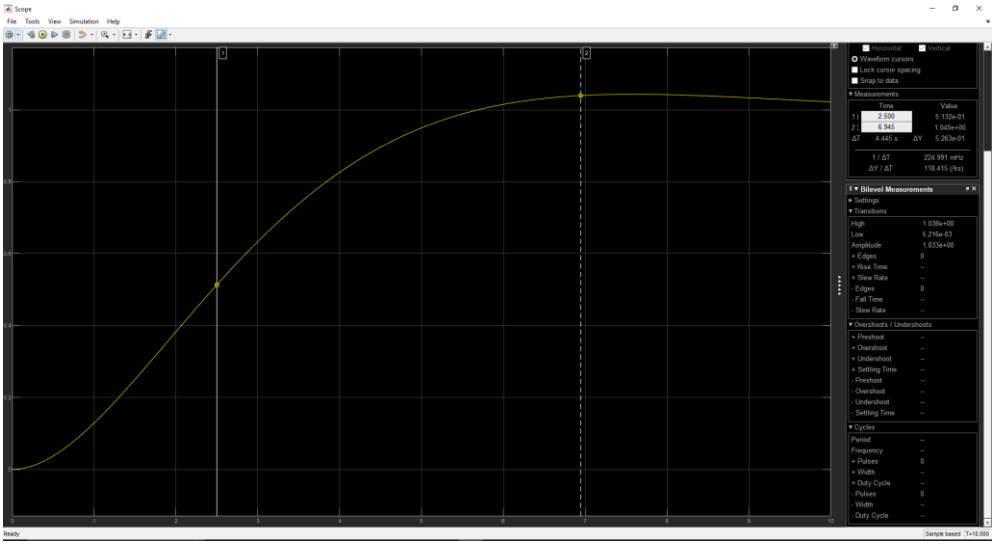

Figure 10. MG-16B DC Motor Response Results Using LQR Method

Figure 10 shows the step response display of the MG-16B LQR DC motor without noise. It can be seen that the step response output of the MG-16B LQR DC motor reaches an amplitude of 1.033 which can be rounded to 1 so that it has reached the setpoint. It has a minimum rise time of 3.940 s and has a fairly small overshoot and undershoot of 0%.

3.3. MG-16B DC Motor Response Results Using LQR Method With Noise

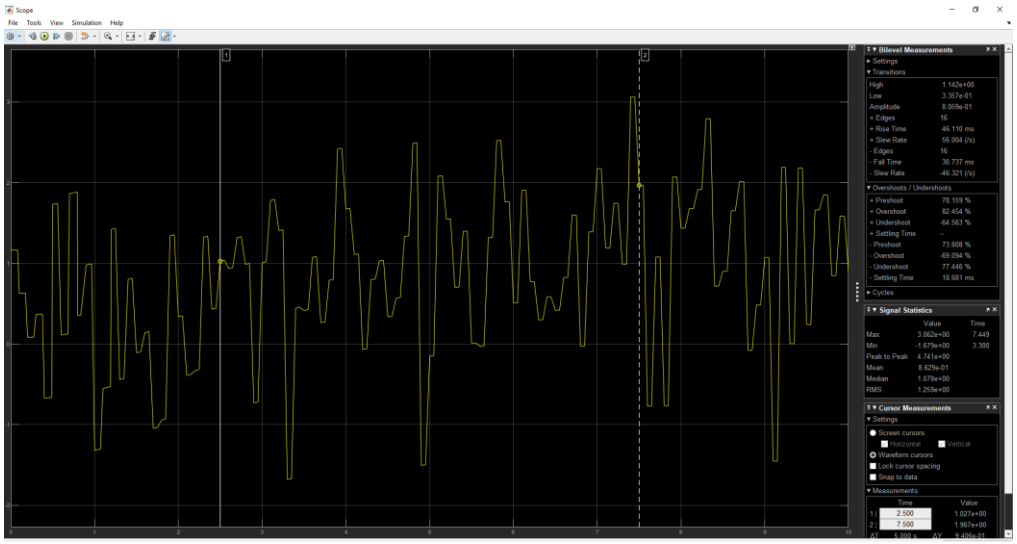

Figure 11. MG-16B DC Motor Response Results Using LQR Method With Noise

Figure 11 shows the step response display of the MG-16B LQR DC motor with noise. It can be seen that the step response output of the MG-16B LQR DC motor only has a fluctuating graph due to the noise given. The system reaches an amplitude of 8.059 so that the system has not

DOI: https://doi.org/10.71225/jstn.v2i3.105

reached the setpoint. It has a fairly maximum rise time at 52.720ms and has an overshoot of 82.454% and an undershoot of -64.563%.

3.4. MG-16B DC Motor Response Results Using LQT Method

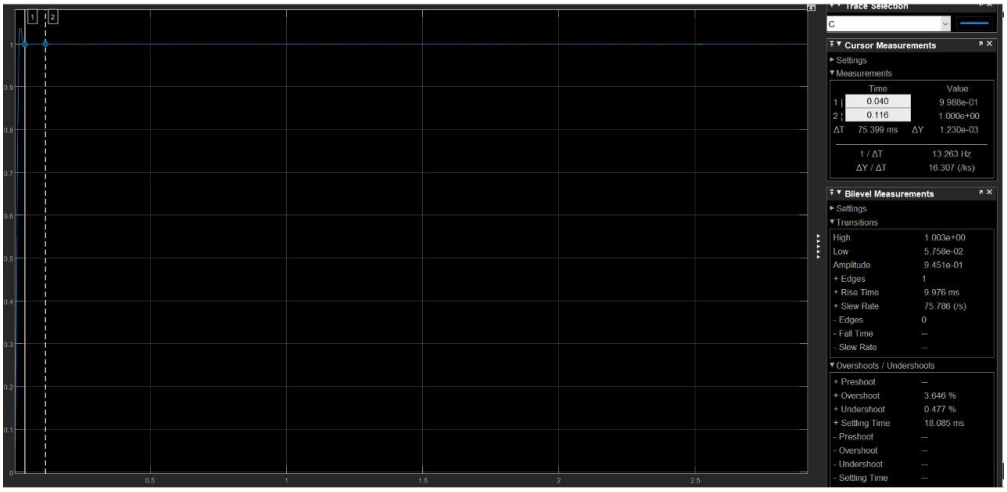

Figure 12. MG-16B DC Motor Response Results Using LQT Method

In the output of the modal response in Figure 12, it can be seen that the response graph of the MG-16B DC motor using LQT has the same output as the desired set point value of 0.5 with a very fast response time to steady state of 8.364us. However, the resulting response has an overshoot of 3.646% and an undershoot of 0.477%.

3.5. MG-16B DC Motor Response Results Using LQT Method With Noise

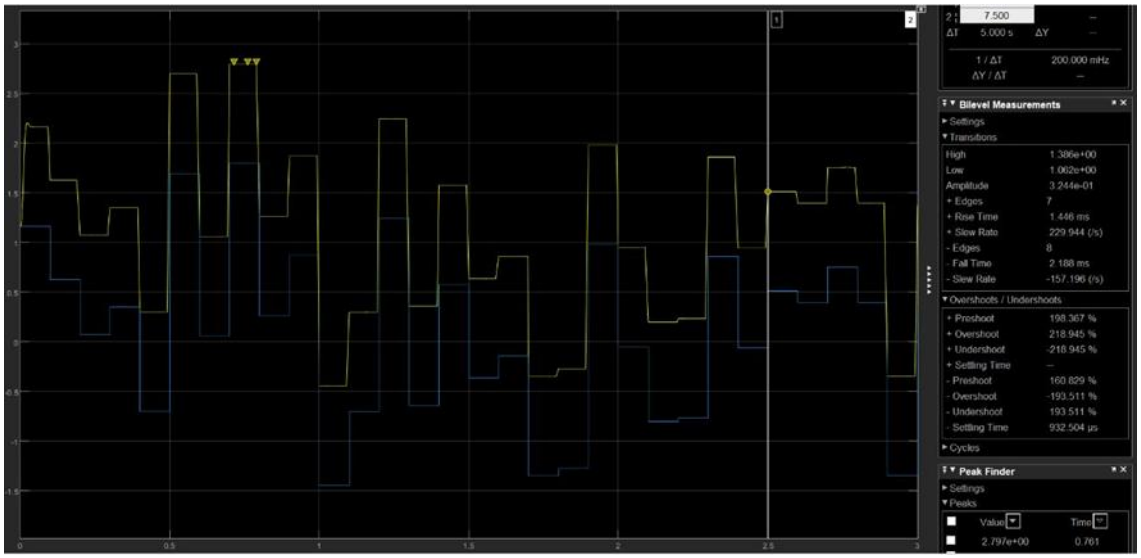

Figure 13. MG-16B DC Motor Response Results Using LQT Method With Noise

From the results of Figure 13, it can be seen that the yellow signal which is the result of the response of the MG-16B DC motor with the LQT method has changed shape from before the noise was given. The signal shape experiences a lot of ripples and imitates the shape of the noise signal

DOI: https://doi.org/10.71225/jstn.v2i3.105

given. The resulting signal is no longer linear and far from stable conditions or steady state at the given set point.

4. Conclusion

Experimental results from the MG-16B DC motor demonstrate that applying the LQR method yields a system response that precisely matches the desired setpoint, without any overshoot or undershoot. The system reaches steady state approximately 1.2 seconds faster compared to operation without the LQR controller. In the absence of LQR, the motor's response deviates significantly from the target value and requires more time to stabilize. However, when noise is introduced into the system, the response of the MG-16B DC motor using LQR tends to follow the noise signal, resulting in a nonlinear output. In contrast, when the LQT method is applied, the motor reaches steady state in just 8.364 microseconds, a notably faster response. Nonetheless, the system experiences an overshoot of 3.646% and an undershoot of 0.477%. Similar to LQR, the motor's output under LQT also follows the noise input, making the system behavior nonlinear when disturbances are present. Despite these imperfections, LQT is considered more advantageous than LQR due to its faster response time in reaching the setpoint for the MG-16B DC motor.

Acknowledgements

The authors gratefully acknowledge the support from the Department of Marine Electrical Engineering and the Department of Design and Manufacture Engineering, Shipbuilding Institute of Polytechnic Surabaya, Indonesia, as well as the Department of Bio-Industrial Mechatronics Engineering, National Chung Hsing University, Taiwan, for their contributions to this research.

References

[1] Nugraha, Anggara Trisna, and Rachma Prilian Eviningsih. Penerapan Sistem Elektronika Daya: AC Regulator, DC Chopper, dan Inverter. Deepublish, 2022.

[2] Nugraha, Anggara Trisna, et al. Rancang Bangun Ship Alarm Monitoring (SAM) Sebagai Solusi Keamanan Pengoperasian Auxiliary Engine. Deepublish, 2021.

[3] Saputra, Fahmi Yahya, et al. "Efficiency Of Generator Set On Changes In Electrical Load On Fishery Vessels." MEIN: Journal of Mechanical, Electrical & Industrial Technology 1.2 (2024): 1-4.

[4] Fauzi, Ahmad Raafi, et al. "Performance of Permanent Magnet Synchronous Generator (pmsg) 3 Phase Radial Flux Results Modification of Induction Motor." MEIN: Journal of Mechanical, Electrical & Industrial Technology 1.2 (2024): 5-11.

[5] Amrullah, Muhammad'Ubaid, et al. "rancang bangun monitoring kualitas air tambak udang vaname dengan kontrol paddle wheel berbasis mikrokontroller." Jurnal 7 Samudra 8.2 (2023): 117-122.

[6] Dermawan, Deny, et al. "Pengontrol Kecepatan Respon Motor dengan Pid dan Lqr." Seminar MASTER PPNS. Vol. 8. No. 1. 2023.

[7] Dermawan, Deny, et al. "Kendali Kecepatan Motor Dengan Kontrol Pid Menggunakan Metode Metaheuristik." Seminar MASTER PPNS. Vol. 8. No. 1. 2023.

[8] Wibowo, Muhammad Ferdiansyah, and Anggara Trisna Nugraha. "perencanaan sistem propulsi elektrik pada fast patrol boat 28 meter." Proceedings Conference on Marine Engineering and its Application. Vol. 6. No. 1. 2023.

DOI: https://doi.org/10.71225/jstn.v2i3.105

[9] Agna, Diego Ilham Yoga, Rama Arya Sobhita, and Anggara Trisna Nugraha. "Penyearah Gelombang Penuh 3 Fasa Tak Terkendali dari Generator Kapal AC 3 Fasa." Seminar MASTER PPNS. Vol. 8. No. 1. 2023.
[10] Apriani, Mirna, et al. "Coastal Community Empowerment Recovery of cockle shell waste into eco-friendly artificial reefs in Mutiara Beach Trenggalek Indonesia." Frontiers in Community Service and Empowerment 1.4 (2022).
[11] Prastyawan, Rikat Eka, and Anggara Trisna Nugraha. "penerapan teknologi informasi untuk pembelajaran test of english for international communication preparation." Jurnal Cakrawala Maritim 5.1 (2022): 4-8.
[12] Ainudin, Fortunaviaza Habib, Muhammad Bilhaq Ashlah, and Anggara Trisna Nugraha. "Pengontrol Kecepatan Respon Motor dengan Pid dan Lqr." Seminar MASTER PPNS. Vol. 7. No. 1. 2022.
[13] Sasongko, Adhy, et al. "Estimation of the thrust coefficient of a Quadcopter Propeller using Computational Fluid Dynamics."
[14] Magriza, Rania Yasmin, et al. "Design and Implementation of Water Quality Control in Catfish Farming Using Fuzzy Logic Method with IoT-Based Monitoring System." Jurnal Teknologi Maritim 4.1 (2021): 13-18.
[15] Putra, Z. M. A., Nugraha, A. T., Widiarti, Y., Safaroz, W., & Sobhita, R. A. (2024). Design of Unipolar Pure Sine Wave Inverter with Spwm Method Based On Esp32 Microcontroller As a Support of The Ebt System On Ship. In *E3S web of conferences* (Vol. 473, p. 01008). EDP Sciences.
[16] Sobhita, R. A. (2024, November). Linear Quadratic Regulator (LQR) and Linear Quadratic Tracking (LQT) control systems on M66 Series DC motors. In *Conference of Electrical, Marine and Its Application* (Vol. 3, No. 1, pp. 1-10).
[17] Fambudi, J. S., & Sobhita, R. A. (2024). Design and Analysis of a Thyristor-Based Controlled Rectifier Circuit for Stabilization of Speed and Rotation in DC Motors. *Journal of Marine Electrical and Electronic Technology*, *2*(2), 1-7.
[18] Sutrisna, V. H. K., Sobhita, R. A., & Nugraha, A. T. (2024). Comparative Analysis of PID and LQR Controllers for Speed Regulation of Series DC Motors. *Journal of Marine Electrical and Electronic Technology*, *2*(2), 1-9.
[19] Santosa, A. F., Sobhita, R. A., & Nugraha, A. T. (2023). Optimization of DC Motor 80BL Using LQR Methods on MATLAB Simulink for Community Empowerment Applications. *Maritime in Community Service and Empowerment*, *1*(1), 1-8.
[20] *Amrullah, Muhammad'Ubaid, et al. "*rancang bangun monitoring kualitas air tambak udang vaname dengan kontrol paddle wheel berbasis mikrokontroller.*" Jurnal 7 Samudra 8.2 (2023): 117-122.*

DOI: https://doi.org/10.71225/jstn.v2i3.105